CENTER FOR CONNECTED AND AUTOMATED TRANSPORTATION

Final Report #ICT-23-015
August 2023

Pavement Distresses Due to Truck Platoons: A Holistic Analysis

Imad L. Al-Qadi
Hasan Ozer
Aravind Ramakrishnan
Ashraf Alrajhi

ILLINOIS CENTER FOR TRANSPORTATION

DISCLAIMER

Funding for this research was provided by the Center for Connected and Automated Transportation under Grant No. 69A3551747105 of the U.S. Department of Transportation, Office of the Assistant Secretary for Research and Technology (OST-R), University Transportation Centers Program. The contents of this report reflect the views of the authors, who are responsible for the facts and the accuracy of the information presented herein. This document is disseminated under the sponsorship of the Department of Transportation, University Transportation Centers Program, in the interest of information exchange. The U.S. Government assumes no liability for the contents or use thereof.

Suggested APA Format Citation:

Al-Qadi. I.L., Ozer, H., Ramakrishnan, A., & Alrajhi, A. (2023). *Pavement distresses due to truck platoons: A holistic analysis* (Report No. ICT-23-015). Illinois Center for Transportation. https://doi.org/10.36501/0197-9191/23-015

Contacts

For more information:

Imad L. Al-Qadi
University of Illinois Urbana Champaign
1207 Newmark Civil Engineering Bldg
alqadi@illinois.edu
https://ict.illinois.edu

CCAT
University of Michigan Transportation Research Institute
2901 Baxter Road
Ann Arbor, MI 48152
uumtri-ccat@umich.edu
(734) 763-2498
www.ccat.umtri.umich.edu

TECHNICAL REPORT DOCUMENTATION PAGE

1. Report No.	2. Government Accession No.	3. Recipient's Catalog No.
ICT-23-015	N/A	N/A

4. Title and Subtitle	5. Report Date
Pavement Distresses Due to Truck Platoons: A Holistic Analysis	August 2023
	6. Performing Organization Code N/A

7. Authors	8. Performing Organization Report No.
Imad L. Al-Qadi (https://orcid.org/0000-0002-5824-103X), Hasan Ozer (https://orcid.org/0000-0003-1526-6840), Aravind Ramakrishnan (https://orcid.org/0000-0003-3269-015X), Ashraf Alrajhi (https://orcid.org/0000-0003-4851-0336)	ICT-23-015 UILU-ENG-2023-2015

9. Performing Organization Name and Address	10. Work Unit No.
Illinois Center for Transportation Department of Civil and Environmental Engineering University of Illinois at Urbana-Champaign 205 North Mathews Avenue, MC-250 Urbana, IL 61801	N/A
	11. Contract or Grant No. Grant No. 69A3551747105

12. Sponsoring Agency Name and Address	13. Type of Report and Period Covered
Center for Connected and Automated Transportation University of Michigan Transportation Research Institute 2901 Baxter Road Ann Arbor, MI 48152	Final Report
	14. Sponsoring Agency Code

15. Supplementary Notes

Funding under Grant No. 69A3551747105 U.S. Department of Transportation, Office of the Assistant Secretary for Research and Technology (OST-R), University Transportation Centers Program.
https://doi.org/10.36501/0197-9191/23-015

16. Abstract

Currently, AASHTOWare PMED does not contain a framework to compute distresses for loading scenarios like truck platoons. Truck platoons reduce fuel consumption and improve safety while increasing pavement damage because of a reduction in wander and rest period. The important parameters of truck platoons are wander, rest period, and penetration level. Unlike wander, the effect of reduced rest period on permanent deformation and platoon penetration level are not well documented. Rest period (i.e., truck spacing) is a critical parameter in platoons that can be controlled to reduce damage or to improve fuel savings. Unlike fatigue cracking, shorter rest periods resulted in lower permanent deformation through conventional repeated load triaxial testing. However, the test does not entail a representative load stress pulse because of moving loads. This study uses modified triaxial testing equipment to simulate different load pulses. Reduced triaxial compression was critical over the conventional load stress pulse. For all representative pulses, the effect of rest period was similar (i.e., increasing rest period increased permanent deformation). The researchers developed a framework to compute pavement distresses as a function of truck platoon parameters. Truck platoons distributed uniformly on sublanes resulted in the lowest damage, even lower than a conventional trucking operation. Truck spacing of 60 ft is optimal in terms of safety, as the difference in distresses were minimal compared to spacing at 18 ft.

17. Key Words	18. Distribution Statement
Truck Platooning, Platoons, Rest Period, Wander, Penetration Level, Pavement Distress, Mechanistic Framework, Repeated Load, Permanent Deformation	No restrictions. This document is available through the National Technical Information Service, Springfield, VA 22161.

19. Security Classif. (of this report)	20. Security Classif. (of this page)	21. No. of Pages	22. Price
Unclassified	Unclassified	33	N/A

ACKNOWLEDGMENT, DISCLAIMER, MANUFACTURERS' NAMES

This project was conducted in cooperation with the Center for Connected and Automated Transportation and the Illinois Center for Transportation. The contents of this report reflect the view of the authors, who are responsible for the facts and the accuracy of the data presented herein. The contents do not necessarily reflect the official views or policies of CCAT or ICT. This report does not constitute a standard, specification, or regulation. Trademark or manufacturers' names appear in this report only because they are considered essential to the object of this document and do not constitute an endorsement of the product by CCAT or ICT.

TABLE OF CONTENTS

LIST OF FIGURES

LIST OF TABLES

CHAPTER 1: INTRODUCTION

The current pavement design methodology, AASHTOWare PMED, does not account for scenarios involving truck platoons. Platoons are expected to have reduced spacing and wander (i.e., channelized) between trucks. Several studies quantified the impacts of truck platoons on pavement distresses and found that platooning accelerates the progression of distresses (Fagnant & Kockelman, 2015; Gungor & Al-Qadi, 2020; Liang et al., 2016). Truck platoons may accelerate pavement damage or reduce pavement life because of channelized traffic, resulting in higher maintenance and rehabilitation costs (Gungor & Al-Qadi, 2022). The impact of lateral spacing of trucks was studied widely in the literature, and a consensus is that reducing wander results in higher distresses (Epps et al., 2002; Gungor & Al-Qadi, 2022; Noorvand et al., 2017). Similarly, the effect of rest period on fatigue was widely studied, and studies found that increasing rest period (i.e., truck spacing) reduces fatigue cracking (Daniel & Kim, 2001; Kim & Roque, 2006; Kim et al., 2001; Underwood & Zeiada, 2014). However, the effect of rest period on rutting was studied, and lower rest period (i.e., truck spacing) results in lower permanent deformation (i.e., rutting) (Alrajhi et al., 2022; Motevalizadeh et al., 2018). However, the impact of truck platoons may vary significantly under realistic operating conditions with varying pavement structures, materials, and environmental factors.

Permanent deformation experiments were used successfully to quantify the impact of rest period on rutting and provided input to the development of a mechanistic prediction model (Ramakrishnan et al., 2021). Permanent deformation experiments using a conventional repeated load are designed based on the most critical stress state, where a given pavement unit under the load is under pure vertical compression without any shear. However, an actual moving truck load impacts a fixed pavement unit differently while approaching, passing, or departing. For example, the stresses on a fixed point are in a triaxial state (vertical, horizontal, and shear) and vary with time as a truck moves over pavement, as presented in Figure 1. The shape and magnitude of moving load stress pulses vary, depending on pavement structure and temperature. Stress states resulting from varying stress paths due to moving loads within the asphalt and base layers impact deformation behavior and rutting performance of pavements. These stress paths include compression, shear, or extension stresses with varying magnitude and orientation of principal stresses depending on the position of loading and depth from the surface.

Although confined or unconfined uniaxial compression stress states capture one of the loading cases within the asphalt concrete (AC) layer, these types of experiments may not represent the most critical stress states or neglect the effect of loading path history because of the passing of vehicles. This study explores alternative stress paths and compares them to conventional repeated load compression stress path tests. Using the alternative stress paths, the significance of stress path on determining the overall permanent deformation resistance of AC mixtures and criticality of various stress paths was explained. Additionally, the tests will verify the impact of rest period using a more representative simulation of moving truck loads in a platoon. Therefore, actual permanent deformation, developed because of moving trucks, may be understood qualitatively.

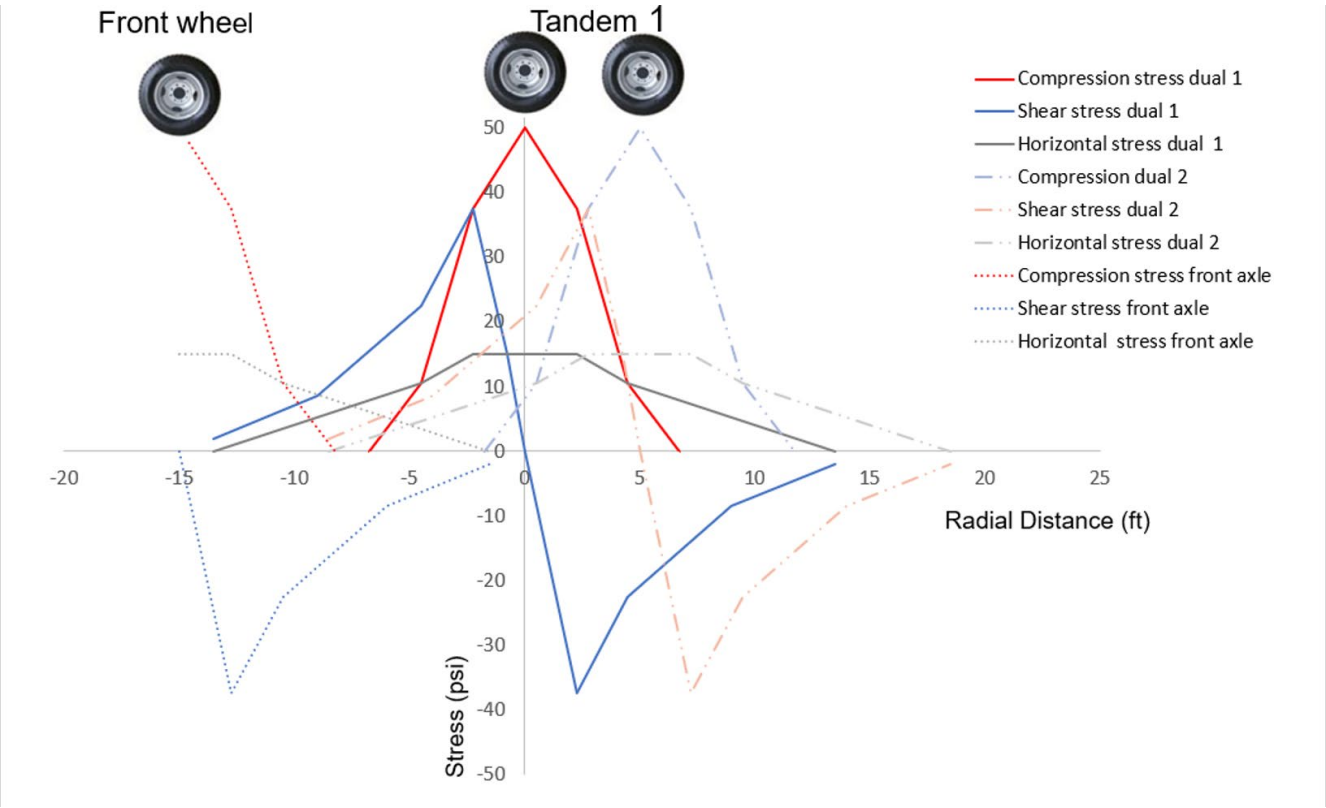

Figure 1. Illustration. Moving load stresses due to steering and first tandem axle of a class 9 truck.

The effect of rest period on pavement damage was studied using an advanced, mechanistic finite element (FE) model and experimental data in the previous University Transportation Center funding cycle. The effect of lateral position and rest period will be combined as a single framework to incorporate in pavement design. Practically, 100% autonomous truck traffic is not possible in the near future. Hence, this study also aims to fill this gap by computing pavement damage as a function of various penetration levels, truck spacing, and wander. This step will be achieved using robust 3D FE pavement model simulations and an experimental program that simulates actual loading scenarios.

OBJECTIVE AND SCOPE

The main goal of the study is to understand the effect of truck platoons qualitatively and quantitatively on pavement distresses. Understanding the effect of stress paths' (i.e., representative loading) impact on permanent deformation and platoon penetration levels will help design future pavements. The work presented in this report is an outcome of collaborative research conducted by the University of Illinois Urbana-Champaign and Arizona State University as part of the Center for Connected and Automated Transportation. The work is sponsored by the U.S. Department of Transportation's University Transportation Center at the University of Michigan. This research project aims to understand qualitatively the impact of rest period using representative loads in experiments as well as to develop a framework to quantify the effect of truck platoons on pavement distresses as a function of rest period, wander, and penetration levels.

The research scope included repeated load deformation tests using custom-designed triaxial equipment and a framework to quantify the distresses. A laboratory-produced AC mixture prepared with modified and unmodified binder was used in the experimental program. Specific research objectives were as follows:

- Quantify the impact of different stress paths representing triaxial compression, triaxial simple shear, and triaxial extension on permanent deformation.
- Assess the impact of rest periods on each stress path.
- Evaluate the comparative performance of modified and unmodified binder.
- Quantify the pavement distresses caused by regular truck traffic and truck platoons at various penetration levels that incorporate both wander and rest period.

CHAPTER 2: IMPACT OF REALISTIC LOADING OF PERMANENT DEFORMATION BEHAVIOR ON ASPHALT CONCRETE

BACKGROUND

Several laboratory test methods were developed to characterize permanent deformation of AC mixtures and to predict rutting in asphalt layers (AASHTO T 378-17, 2017; Gibson et al., 2003; Uzan, 2003; Witczak et al., 2002; Zhang et al., 2002; Zhou et al., 2004). As part of the National Cooperative Highway Research Project 9-19, the flow number and flow time tests were developed as a simple performance test using repeated axial load applications and a constant confinement pressure (AASHTO T 378-17, 2017; Witczak et al., 2002). A main assumption made with the use of the flow number test was that the critical state for permanent deformation was when axial compression was applied through the vertical axis of a cylindrical specimen. The tests were conducted at a typical axial stress state representing the structure and representative site temperature. The triaxial stress sweep test was developed more recently to account for the effect of temperature, loading time, and axial stress state (Choi & Kim, 2013; Kim & Kim, 2017). Both test methods consider the triaxial compression state applied through the vertical axis of a cylindrical specimen—in other words, the major principal axis. These test methods formed the basis of mechanistic rutting performances in their respective platforms (Choi & Kim, 2013; Kim & Kim, 2017; Witczak, 2007; Witczak et al., 2002).

Advanced permanent deformation tests of AC mixtures were also developed with a goal to predict rutting in asphalt layers using numerical methods (Choi & Kim, 2013; Darabi et al., 2013; Subramanian et al., 2013). The stress states used in these tests are more complicated and designed to derive parameters of viscoelastic and viscoplastic constitutive relationships. Blocks of repeated axial deviatoric stresses with variable loading, unloading time, and stress magnitude were applied at a constant confining pressure representative of a stress state in AC layers. The outcome of the tests was used successfully for implementation of a viscoplastic constitutive relationship in a FE analysis program (Abu Al-Rub et al., 2012; Darabi et al., 2019; Rahmani et al., 2013; Shakiba et al., 2017). Similar to the simple performance tests, these advanced permanent deformations also assumed the triaxial compression state on a cylindrical specimen as the critical condition for AC layers and mixes.

In contrast, the effect of stress paths other than triaxial compression was studied to evaluate the level of anisotropy on the resilient modulus and permanent deformation characteristics on granular (i.e., unbound) materials (Ashtiani, 2009; Kim & Tutumluer, 2005). Kim and Tutumluer (2005) and Ashtaini (2009) investigated the impact of changing stress paths owing to moving wheel loads on permanent deformation of granular materials. The stress paths studied included constant confinement pressure stress and variable dynamic confining pressure applied on both vertical and horizontal axes simultaneously. The studies demonstrated that the change of stress paths could produce higher permanent deformation in granular layers compared to traditional unconfined or confined repeated load triaxial compression tests.

Rutting prediction models for AC layers are solely dependent upon confined or unconfined repeated load compression testing (Kim & Kim, 2017; Witczak & El-Basyouny, 2004; Witczak et al., 2002).

Despite some differences between the simple performance test and the stress sweep test (such as flow number), all existing permanent deformation experiments used for AC mixtures assume the triaxial compression state as the most critical state. However, AC layers are subjected constantly to varying stress states because of moving loads, which can drastically change a layer's resistance to permanent deformation. At a given fixed point, the magnitude of horizontal and axial stresses varies with respect to depth from surface and load position. If the AC mixture also shows some degree of anisotropy, then the variable stress paths may result in substantially different permanent deformation characteristics than the triaxial compression stress path. Thus, there is a need to understand AC mixtures' responses to permanent deformation using stress paths other than conventional triaxial compression repeated load tests.

This research presents experimental results, demonstrating the impact of various stress paths on permanent deformation resistance of AC mixes prepared with modified and unmodified asphalt binder. The stress paths included are triaxial compression, triaxial simple shear and triaxial extension enabled by a custom-designed triaxial testing equipment capable of independently applying vertical deviatoric stress pulses, and horizontal static and dynamic confining stresses. Each stress path represented different loading positions at various depths from the surface. In addition, variable pulse configurations were designed to include variation in rest periods. The most critical stress path for permanent deformation was identified. The outcomes of this research can be implemented in the revision of rutting prediction models for design purposes or can contribute to plasticity-based constitutive relationships. In addition, with the introduction of truck platoons, a fundamental understanding of permanent deformation behavior is needed under variable stress paths with unloading or rest periods considered a variable. Previous work demonstrated the effect of rest period on AC permanent deformation under the unconfined compression state (Alrajhi et al., 2022; Ramakrishnan et al., 2021). As there may not be any field observations in the near future when truck platoons penetrate the freight industry, a realistic prediction of rutting in AC layers can be made for pavements that will be subjected to loading configurations from this new technology.

STRESS STATE AND PATH DEFINITIONS

Stress state is a fixed position and depth from the pavement surface because of moving loads or static loads. Stress states are often represented by the Mohr Circle approach, which is a graphical approach calculating stresses in different planes by reducing them to vertical and horizontal components (Holtz et al., 1981; Lambe & Whitman, 1991; Meyers & Chawla, 2008). As an alternative, the same stress states can be defined in the p-q plane. The mean stress component is represented by the p-axis, and the deviatoric stress component is represented by the q-axis. The graphical Mohr Circle approach was effectively used to visualize the relationships between shear and normal stresses on any plane. Equations presented in Figure 2, Figure 3, Figure 4, and Figure 5 can be used to capture a stress path at any given slope.

$$q = \sigma_1 - \sigma_3$$

Figure 2. Equation. Calculation of the deviatoric stress.

$$p = \frac{(\sigma_1 + 2\sigma_3)}{3}$$

Figure 3. Equation. Calculation of the average of principal stresses.

$$m = \frac{\Delta q}{\Delta p}$$

Figure 4. Equation. Calculation of the slope of a stress path.

$$L = \sqrt{(p^2 + q^2)}$$

Figure 5. Equation. Calculation of the length of a stress path.

where q = deviatoric stress, p = average of principal (normal) stresses (σ_1, σ_3), m = slope of stress path, L = length of stress path, Δq = change of deviatoric stresses from q_s (major/minor principal stresses owing to overburden) to q_{max} (major/minor principal stresses owing to moving load stresses), Δp = change of average normal stresses from p_s (major/minor principal stresses owing to overburden) to p_{max} (major/minor principal stresses owing to moving load stresses).

Stress paths can be defined to represent varying states of stress as a function of time or changing position of loads. Stress path analysis is commonly applied for experimental characterization of plastic deformation for soils and foundations. Stress paths indicate the loading history of a point subjected to various magnitudes of major and minor principal stresses acting on planes with varying degree of rotation from cartesian coordinate systems. The most commonly used stress paths in the analysis of soils and granular materials include hydrostatic compression (Case A), conventional triaxial compression (Case B), simple shear (Case C), reduced triaxial compression (Case D), and conventional triaxial extension (Case E) (Ashtiani, 2009; Lambe & Whitman, 1991). These stress paths are developed by changing horizontal and confining pressure independently, as presented Figure 6. As it is convenient to define stress paths in the p-q plane, Figure 7 illustrates the abovementioned stress paths in the p-q plane.

Path A: Hydrostatic Compression Stress Path

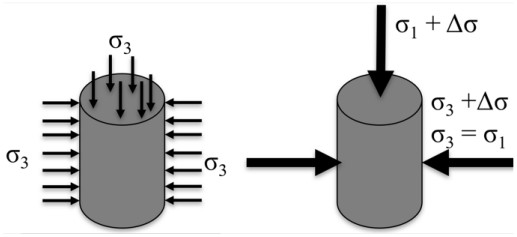

$\Delta\sigma_h = \Delta\sigma_v$

σ_1 and σ_3 increases with the same magnitude.

A. Hydrostatic compression stress path

Path B: Conventional Triaxial Compression Stress Path

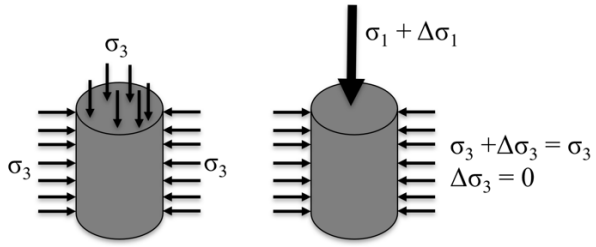

$\Delta\sigma_h = 0$, positive $\Delta\sigma_v$
σ_1 increases, σ_3 remains constant.

B. Conventional triaxial compression stress path

Path C: Simple Shear Stress Path

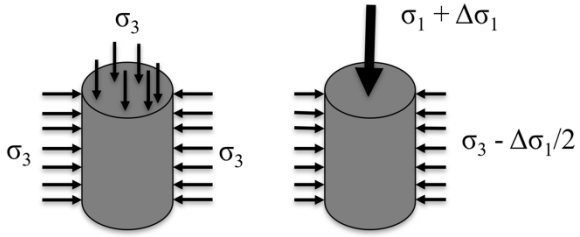

$$\Delta\sigma_h = \frac{-\Delta\sigma_v}{2}$$

Any increase in the σ_1 is corresponded by half the amount of decrease in theσ_3.

C. Simple shear stress path

Path D: Reduced Triaxial Compression Stress Path

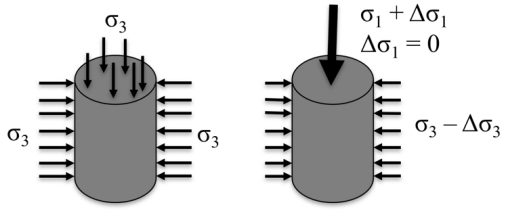

Negative $\Delta\sigma_h$, $\Delta\sigma_v = 0$
σ_1 remains constant and σ_3 decreases.

D. Reduced triaxial compression stress path

Path E: Conventional Triaxial Extension Stress Path

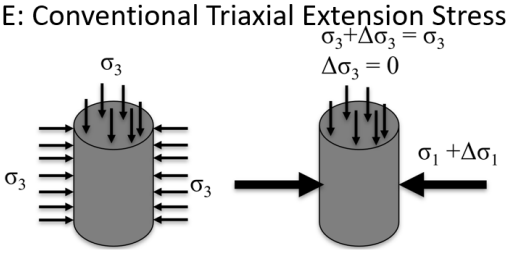

Positive $\Delta\sigma_h$(increases), $\Delta\sigma_v = 0$
σ_1 remains constant and turn into the minor principal stress σ_3 increases and turn into the major principal stress.

E. Conventional triaxial extension stress path

Figure 6. Illustration. Summary of commonly used stress paths in the development of triaxial test for soils and granular materials.

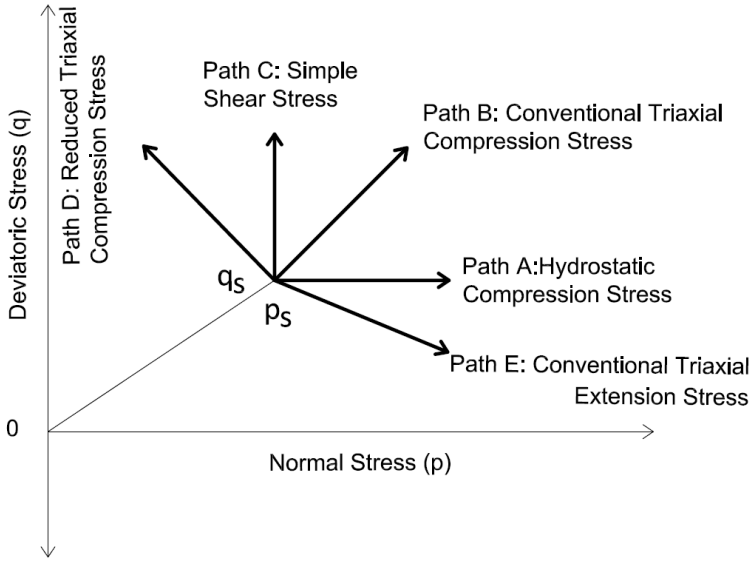

Figure 7. Plot. Stress paths in the p-q plane.

Source: Holtz et al. (1981); Lambe & Whitman (1991)

EXPERIMENTAL PLAN AND MATERIALS

Materials and Mix Design

The aggregate source selected in this research was a granite type that was provided by a local producer in Phoenix, Arizona. A 1/2-in fine-graded mix was reproduced in the laboratory. Aggregate stockpile percentages are as follows: 18.5% of 3/4-in coarse aggregate, 17% of 3/8-in coarse aggregate, 18% of crusher fine, 30% of clean crusher fine, 15% of concrete sand, and 1.5% of type II cement. The testing specimens were produced using PG 70-10, PG 64-22, and PG 76-22 SBS binders. Two unmodified binders and one modified binder were selected to assess the impact of binder modification, recognizing the significance of life-cycle implications of binder selection on mixture performance (Praticò et al., 2011). Table 1 presents a summary of the volumetric properties of the mix design parameters, and Figure 8 presents the aggregate blend gradation in the mix.

Table 1. Composite Aggregate Properties for the Fine-Graded Mix

Volumetric Property	Value	Specification
Asphalt Binder Type	PG 70-10, PG 64-22, and PG 76-22 SBS	N/A
Target Asphalt Content (%)	5.7	N/A
Bulk Specific Gravity (G_{mb})	2.361	N/A
Theoretical Max. Specific Gravity (G_{mm})	2.455	N/A
Percent Air Void	3.8	3.8–4.2
Percent Voids in Mineral Aggregate (VMA)	15.5	14 min.
Percent Voids Filled with Asphalt (VFA)	75.3	N/A
Dust Ratio	1.0	0.6–1.4

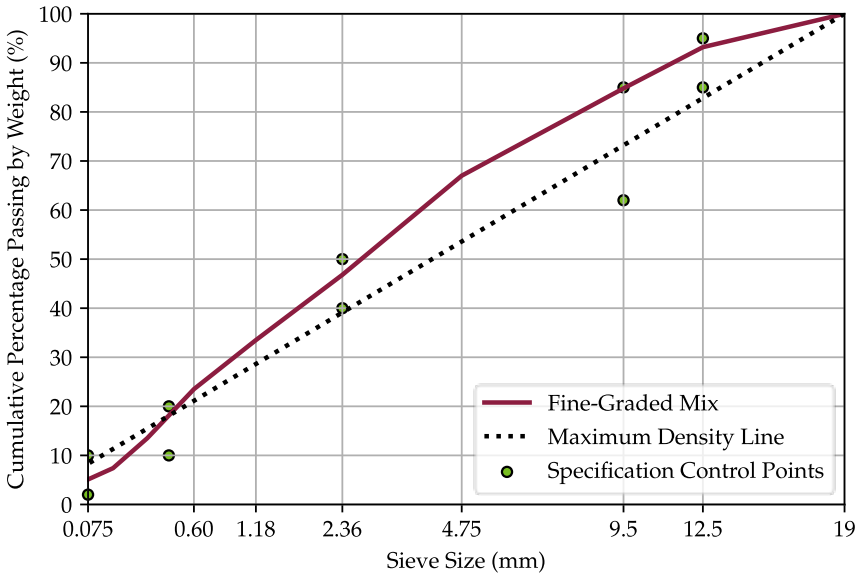

Figure 8. Graph. Aggregate gradation for a dense, fine-graded mix design.

Experimental Program

The first phase of the experimental plan included conventional repeated-load permanent deformation tests with confining pressure at different temperatures. The capabilities of the custom-designed triaxial testing equipment were verified and benchmarked with trends obtained in earlier work, and the impact of rest period on viscoelastic and viscoplastic deformation was explored (Alrajhi et al., 2022). In the second phase, three stress paths were designed, as presented in Figure 6. Stress path B is the commonly used conventional triaxial compression path with a slope of 3.0. The other stress paths included simple shear stress path C with an infinite slope and reduced triaxial compression stress path D with a slope of −1.5. The stress paths are illustrated in Figure 9 and Figure 10. The stress matrix used in the experiments is introduced in Table 2, Table 3, and Table 4. The stress paths were applied on specimens prepared with PG 70-10 and PG 76-22 SBS at 130°F and prepared with PG 64-22 at 104°F. Axial deviatoric stresses were applied using a pulse configuration with 0.05-second loading time and two rest periods (0.18 and 2.5 seconds). The two rest-period scenarios were considered to simulate spacing distances between trucks: 0.18 seconds corresponded to 16 ft—the shortest spacing between any two trucks of a platoon, whereas 2.5 seconds corresponded to 220 ft as a typical safe sight distance between trucks. Static confinement pressure was applied.

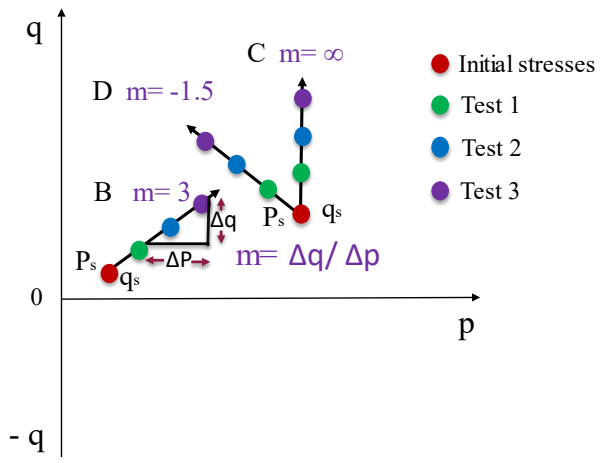

Path B: Conventional Triaxial Compression Stress Path: $\Delta\sigma_h = 0$ and $\Delta\sigma_v$ increases
Path C: Simple Shear Stress Path: $\Delta\sigma_h = -\Delta\sigma_v$
Path D: Reduced Triaxial Compression Stress Path: $\Delta\sigma_h$ decreases and $\Delta\sigma_v = 0$

$q = \sigma_1 - \sigma_3$

$p = (\sigma_1 + 2\sigma_3)/3$

where

σ_1 = greatest principal stress (axial stress),
σ_3 = least principal stress (confinement or static stress),
σ_{1d} = axial deviatoric stress, σ_{3d} = horizontal deviatoric stress, initial(p_s , q_s) = initial stress state, test 1= stress state at point 1, test 2= stress state at point 2, test 3= stress state at point 3.

Figure 9. Illustration. Schematic of stress paths used in the experiments.

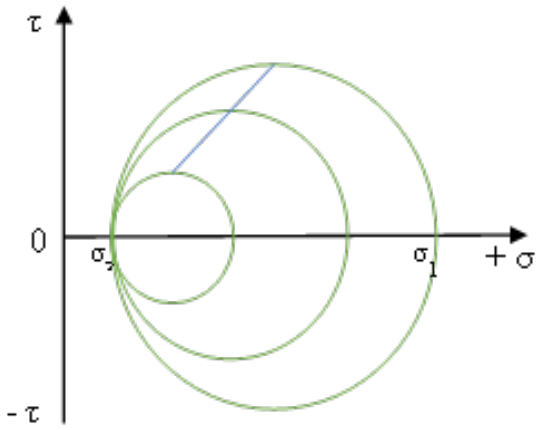

A. Stress path A

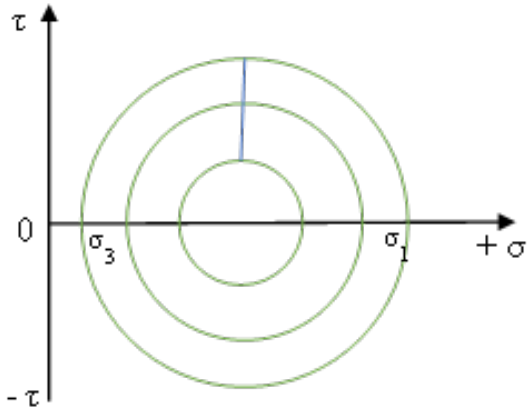

B. Stress path B

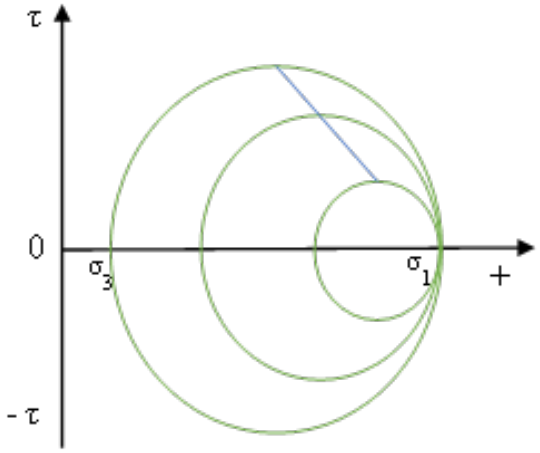

C. Stress path C

Figure 10. Illustration. Stress path demonstration using a Mohr circle diagram.

Table 2. Stress States Used in the Triaxial Compression Path.

Test #	σ_3 (psi)	σ_{1d} (psi)	σ_{3d} (psi)	σ_1 (psi)	p_o (psi)	q_o (psi)	p_{max} (psi)	q_{max} (psi)	m
Initial[1]	10	0	0	10	10	0	–	–	–
Test 1	10	81	0	91	–	–	37	81	3
Test 2	10	110	0	120	–	–	46.7	110	3
Test 3	10	139	0	149	–	–	56.3	139	3

Table 3. Stress States Used in the Simple Shear Path.

Test #	σ_3 (psi)	σ_{1d} (psi)	σ_{3d} (psi)	σ_1 (psi)	p_o (psi)	q_o (psi)	p_{max} (psi)	q_{max} (psi)	m
Initial[1]	35	76.9	0	112.4	61.2	76.9	–	–	–
Test 1	25	107.3	0	132.7	–	–	61.2	107.3	∞
Test 2	15	137.8	0	153	–	–	61.2	137.8	∞
Test 3	5	168.2	0	173.3	–	–	61.2	168.2	∞

Table 4. Stress States Used in Reduced Triaxial Compression Path.

Test #	σ_3 (psi)	σ_{1d} (psi)	σ_{3d} (psi)	σ_1 (psi)	p_o (psi)	q_o (psi)	p_{max} (psi)	q_{max} (psi)	m
Initial[1]	35	137.8	0	173.3	67	137.8	–	–	–
Test 1	25	148	0	173.3	–	–	74.7	148	−1.5
Test 2	15	158.1	0	173.3	–	–	67.9	158.1	−1.5
Test 3	5	168.2	0	173.3	–	–	61.2	168.2	−1.5

[1] Initial testing stage to apply static axial and confinement stresses.

Multi-axial Variable Pressure Triaxial Testing Equipment

Custom-designed triaxial testing equipment was developed to conduct the experiments in this study (Figure 11). The triaxial testing equipment was designed to apply dynamic pulses in the axial and horizontal axes independently. Similar equipment designs were used in the characterization of granular materials (Ashtiani, 2009; Kim & Tutumluer, 2005). A universal testing machine with a 5620.2 Ib hydraulic frame was upgraded with a 24-bit resolution controller and custom-designed triaxial testing system. The new triaxial testing system is capable of applying dynamic pulses in the axial and horizontal directions for 4 in × 6 in and 6 in × 8 in specimens. The system was designed to use water as the confining medium for dynamic pulses and air for static pulses. Maximum confinement pressure can be up to 87 psi. The triaxial system is operated in an environmental

chamber with a temperature range of −4ºF to 158ºF. The system is capable of combining a versatile range of vertical and horizontal pulse configurations to simulate the effects of moving loads. The controller provides flexibility to develop various pulse configurations that can represent the stress paths used in this study as well as more sophisticated ones such as moving load stress states or aircraft braking and turning. Figure 11 presents the triaxial testing equipment and specimen setup.

A. Specimen setup

B. Triaxial testing equipment

Figure 11. Photo. Custom-designed triaxial testing equipment capable of applying multiaxial variable pulses.

Testing Protocol

Samples with a 6-in diameter were compacted to a constant height of 7.0866 in with a Superpave gyratory compactor with a target air void of 7±0.5% following AASHTO T 312. The samples were then cored to 4 in, and the edges were sawed to obtain a final testing specimen of 6-in height in a similar procedure to that of AASHTO T 378. Prior to testing, the samples were conditioned in an environmental chamber to the desired testing temperature. First, static confinement and initial stress were applied (p_s and q_s), depending on the desired stress state to achieve the target stress path. Then, Linear Variable Differential Transformer (LVDTs) were reset, and repeated dynamic axial stresses and horizontal static stresses were applied on the sample simultaneously to achieve the desired stress state for every sample. Testing continued until 20,000 cycles or 0.4 in, whichever came first.

RESULTS AND DISCUSSION

Complex Modulus Characterization

Figure 12 presents the complex modulus results for three binders (PG 64-22, PG 70-10, and PG 76-22 SBS). The mix with PG 64-22 had the lowest modulus across the frequency and temperature spectra. The effect of polymer modification is observed at higher temperatures and lower frequencies. Phase angle and complex modulus is also present with black space and Cole-Cole plots. Phase angles over the temperature-frequency spectrum along with the black space and Cole-Cole plots did not reveal any significant differences to distinguish the three mixes.

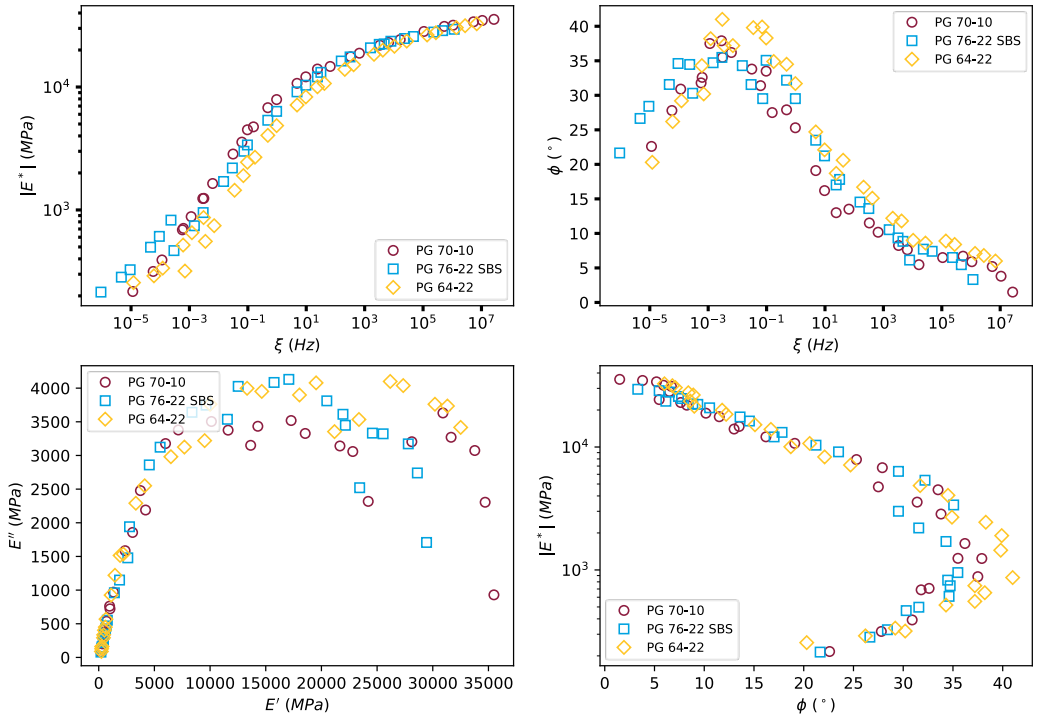

Figure 12. Plot. Complex modulus results.

Effect of Rest Period on Permanent Deformation

The effect of rest period on permanent deformation without confinement was quantified in an earlier study using the repeated load deformation test without confinement (Alrajhi et al., 2022). Increasing the rest period from 0.18 to 2.5 seconds resulted in significant increases in permanent deformation in the range of 70% to 80%. The tests were repeated using the same mix and a similar rest-period range but with the addition of confinement pressure at 10 psi. Figure 13 presents the permanent deformation accumulated in the radial and axial directions for the mix with PG 76-22 SBS at three stress levels as well as short and long rest periods. The increase in permanent deformation with increasing rest period is evident in the results of both axial and radial directions. In addition, the impact of rest period is comparable to a change in the deviatoric stress levels of 29 psi.

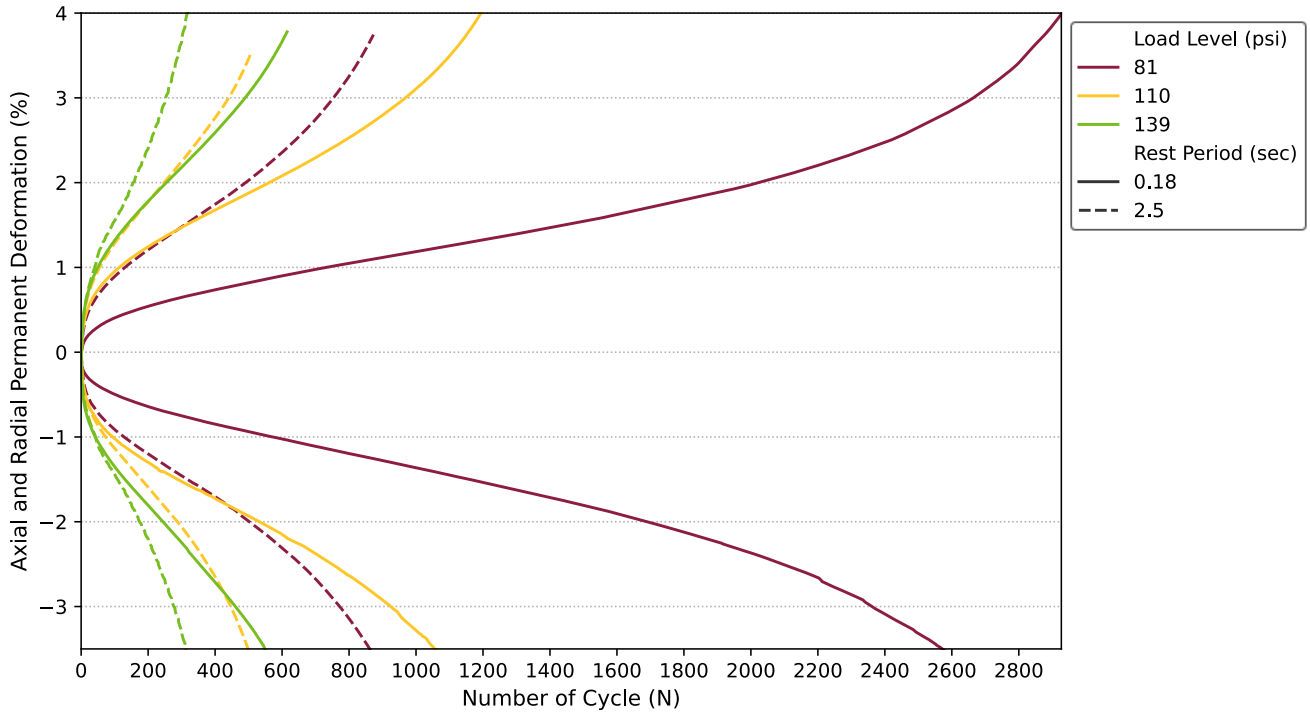

Figure 13. Plot. Effect of rest period with confinement for the PG 76-22 SBS mix at three stress levels and 130°F.

Figure 14 illustrates a comparison of two mixes prepared with PG 76-22 SBS and PG 70-10. An earlier study demonstrated that the PG 76-22 SBS mix has better resistance to permanent deformation by almost three times at 104°F and 130°F (Alrajhi et al., 2022). The results are consistent in the present study with confinement. The comparison also consistently demonstrates that the mix with PG 76-22 SBS tested with a rest period of 2.5 seconds has a comparable permanent deformation trend with the PG 70-10 mix tested with a rest period of 0.18 seconds.

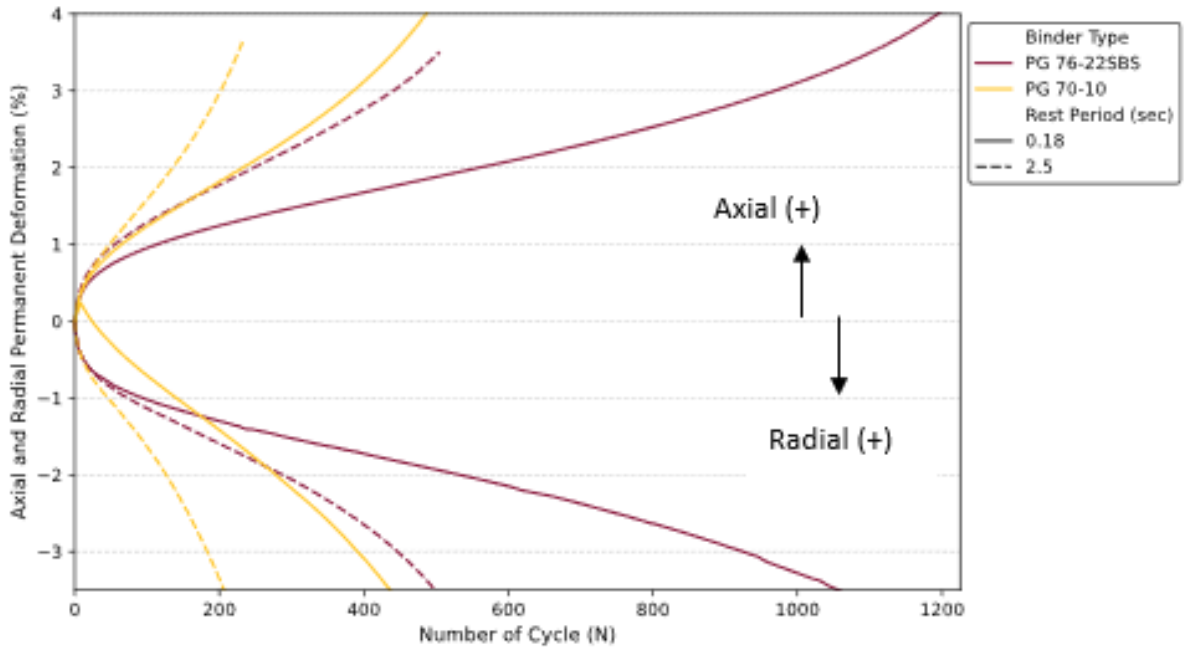

A. Deviatoric stress level of 110 psi

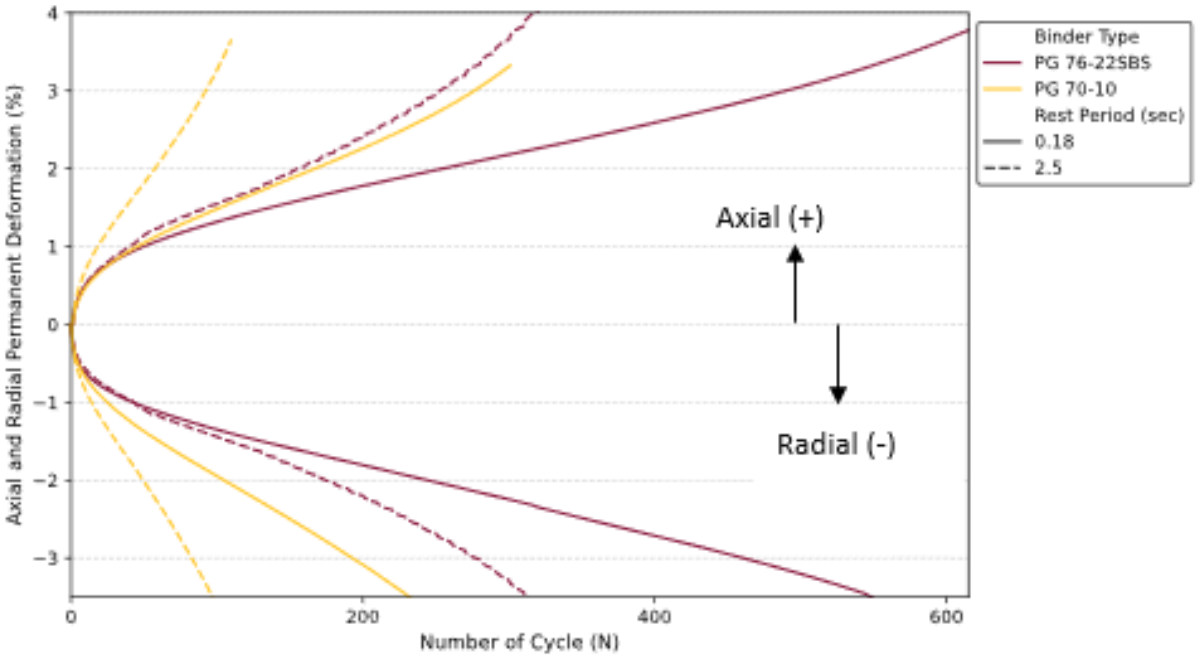

B. Deviatoric stress level of 139 psi

Figure 14. Comparison of mixes with PG 76-22 SBS and PG 70-10 tested at 130°F and different deviatoric stress levels.

Stress Path Analysis

The results from stress paths B, C, and D are discussed. The stress paths were defined as follows:

- Stress path B is the conventional triaxial compression test.
- Stress path C is the simple shear stress path.
- Stress path D is the reduced triaxial compression.

The number of cycles to reach 3.5% of permanent strains were extracted and presented in Figure 15. Stress path D (m = −1.5) required a much lower number of cycles to reach 3.5% strains than stress paths B (m = 3) and C (m =∞). Significantly higher permanent deformation is accumulated for path D compared to path B, which represents conventional repeated load permanent deformation tests. Stress path D is a more critical stress state in terms of permanent strain.

The number of cycles were consistently higher with PG 76-22 SBS binder (almost two to three times higher than those with PG 70-10) at all combinations of stress paths and rest periods. The effect of rest period was also consistent for both binder and stress path. Increasing rest period resulted in almost two to three times higher permanent strain. An increase in rest period from 0.18 seconds to 2.5 seconds had an equivalent impact of changing the binder from PG 76-22 SBS to PG 70-10 (i.e., PG 70-10 at a 0.18-second rest period and PG 76-22 SBS at a 2.5-second rest period).

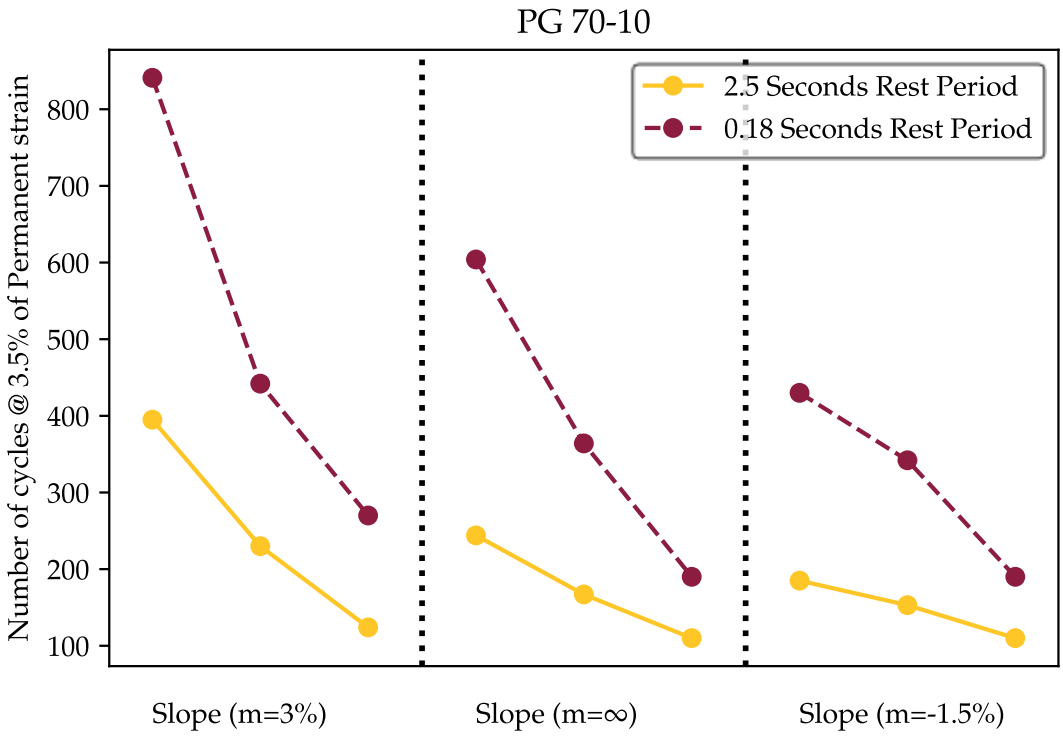

A. PG 70-10

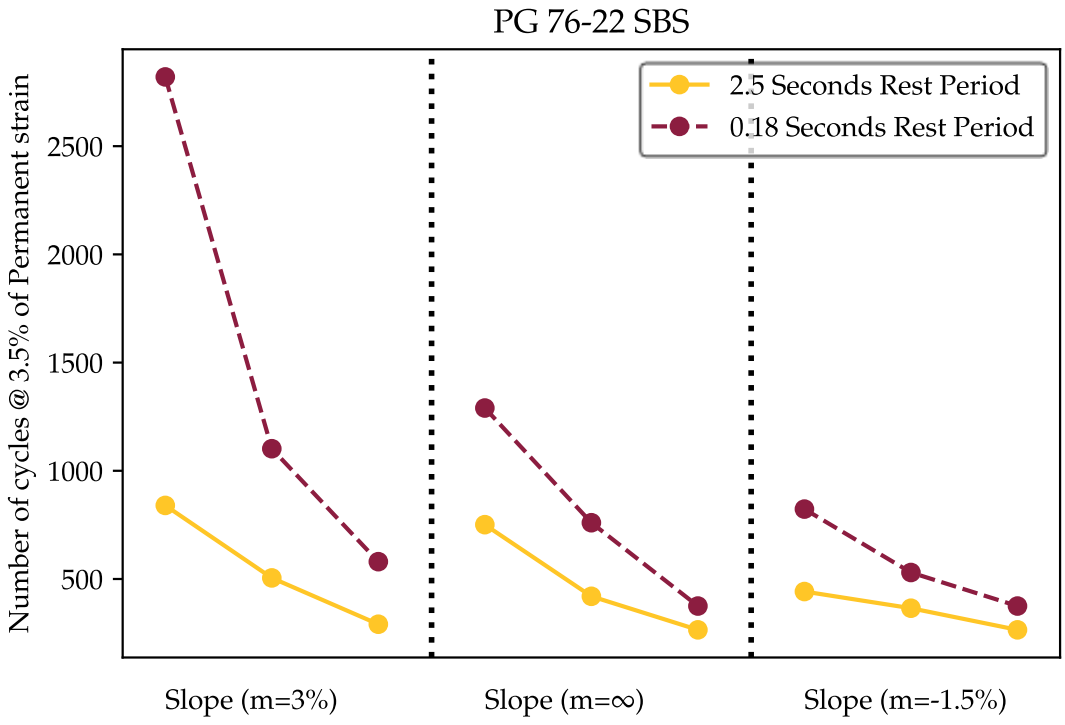

B. PG 76-22 SBS

Figure 15. Effect of stress path for rest periods of 0.18 seconds and 2.5 seconds at 130°F for PG 70-10 and PG 76-22 SBS.

SUMMARY AND CONCLUSIONS

The effect of stress path on permanent deformation characteristics of modified and unmodified AC mixtures was presented. The stress paths included conventional triaxial compression and reduced triaxial compression. Rest period was added to the stress paths as a variable. The mixes were tested using stress states constituting three different stress paths and two temperatures.

Major findings and conclusions are as follows:

- Increasing the rest period from 0.18 to 2.5 seconds at 104°F and 130°F for conventional triaxial tests with static confinement resulted in higher permanent deformation. The results presented in this paper are consistent with results from the previous study (Alrajhi et al., 2022) where no confinement was applied.

- Stress path D (reduced triaxial compression) was found to be the most critical stress state in terms of permanent strain. The number of cycles to reach a critical permanent strain dropped by almost half to one-third with stress path D compared to conventional triaxial stress path B. This is an important observation underscoring the need to account for the variable stress states that pavement layers can be subjected to because of moving loads.

- Increasing rest period consistently increased permanent deformation almost two to three times higher under the three stress paths. The significance of rest period as a testing variable along with stress state and temperature in repeated load permanent deformation tests is once again underlined.

- The mix with PG 76-22 SBS binder demonstrated significantly higher resistance to permanent deformation than the mix with unmodified PG 70-10 at all stress path and rest period combinations.

CHAPTER 3: MECHANISTIC FRAMEWORK FOR COMPUTING PAVEMENT DISTRESSES

Earlier work revised the mechanistic analysis of pavements to include the effects of wander and rest period individually as well as to predict pavement damage with truck platoon operation compared to conventional truck flow (Al-Qadi et al., 2021; Ramakrishnan et al., 2021). A holistic framework is required that incorporates the effect of both rest period and lateral position. This framework would also be useful in determining the optimal platooning strategy that reduces pavement damage while saving fuel consumption. Meanwhile, 100% autonomous truck traffic is not possible practically in the near future. Hence, this framework also aims to fill this gap by computing pavement damage as a function of various penetration levels of platoons.

METHODOLOGY

The methodology can be divided into three parts—namely, 3D FE pavement modeling, an experimental program with shifting curves for rest period, and the inclusion of rest period and wander into the mechanistic-empirical methodology. Each part is summarized in the following subsections.

FE Pavement Model

The current design procedure (AASHTOWare PMED) uses linear elastic analysis to obtain pavement responses with a simplified assumption for tire loading, layer interactions, material properties, and analysis (i.e., static). Al-Qadi and colleagues developed a 3D FE pavement model to overcome the shortcomings of the existing procedure (Al-Qadi & Yoo, 2007; Elseifi et al., 2006; Hernandez et al., 2016; Yoo et al., 2006; Yoo & Al-Qadi, 2007). The developed model can be utilized to obtain pavement responses for any layer configuration, tire loading (i.e., tire type), axle configuration, and material properties.

Experimental Data and Analysis

An experimental program was developed to understand the rest period mechanism on AC permanent deformation. Alrajhi and Ozer (2022) performed repeated load permanent deformation tests for various AC binders, temperatures, loading levels, and rest periods. Permanent deformation was consistently observed to be higher for longer rest periods (Figure 16) irrespective of other parameters in the experimental matrix. A hypothesis, the hardening-relaxation phenomenon, was attributed to explain the behavior.

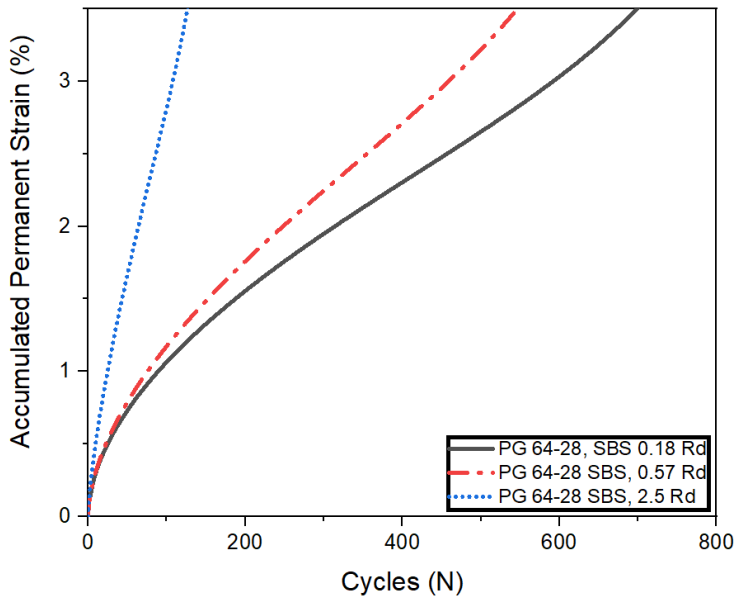

Figure 16. Plot. Effect of rest period on permanent deformation at 140 psi and 104°F.

Source: Alrajhi et al. (2022)

The experimental results of this study were used to quantify the effect of rest period. Using the experimental data, a shift model was developed by extending the principle of the time-temperature superposition framework. Shift factors can be computed using shift function coefficients. The main advantage of the shift model is to predict deformation for the new rest period without running additional tests (Figure 17).

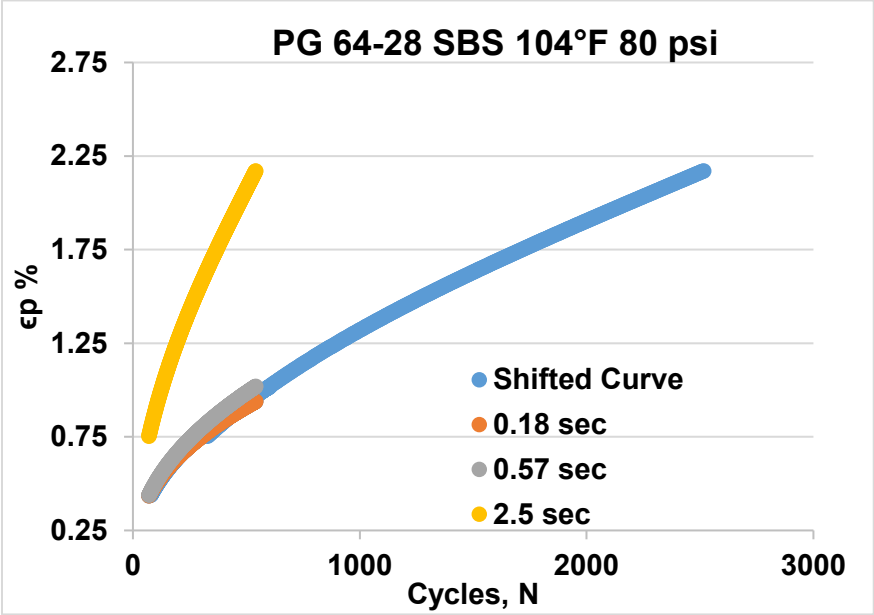

Figure 17. Plot. Shifted curve for experimental data.

Source: Ramakrishnan et al. (2021)

Coefficients of shift functions were developed as a function of stress level and temperature. Using the shift factors, the effect of rest period can be incorporated easily into the PMED procedure by calculating the equivalent load repetitions. Equivalent load repetitions are a form of correction factor that account for the effect of rest period. A detailed procedure of obtaining shifting curves and the correction factor can be found in Ramakrishnan et al. (2021).

Inclusion of Rest Period and Wander

Wander, or the lateral positioning of trucks, was a key parameter in reducing the impact of truck loading, especially in truck platoons. However, the impact of platooning can vary significantly under realistic operating conditions with varying pavement structures, materials, and environmental factors. This study combined the effect of lateral position and rest period as a single framework to incorporate into pavement design. Okte and Al-Qadi (2022) proposed the "Expected Response Framework," which includes the effect of wander and platoon penetration level into the distress calculation (Figure 18). The expected response framework was modified to incorporate the effect of rest period into pavement distress calculations. This framework was selected because of its technical accuracy and lower computational effort. The modified framework can predict distresses for various penetration levels, platoon sizes and spacing (i.e., rest period), different lateral distributions of platoons, and different positions of the platoon.

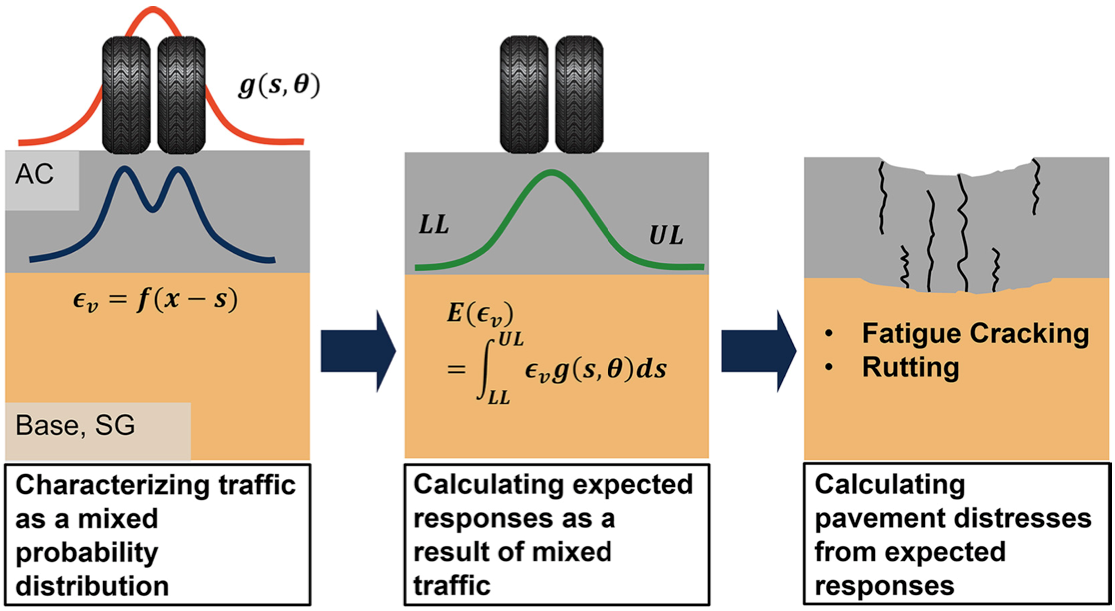

Figure 18. Illustration. Overview of expected response framework.

Source: Okte & Al-Qadi (2022)

CASE STUDY SECTION

The properties of the case study section were obtained using LTPP InfoPave. The closest and most representative section of the corridor was located on I-57 north of Rantoul, Illinois (LTPP Section ID: 17-5849). Inputs such as temperature and annual average daily truck traffic (AADTT) were obtained from the database. Though the section is a composite pavement (PCC overlay), the section was

considered a flexible pavement system. The models used in the structural analysis calculations were verified from permanent deformation experiments conducted on materials representing typical mixes used in two regions. Therefore, the technical approach in this proposed work will aim to predict pavement damage specific to the selected routes and platoon scenarios. The detailed inputs and assumptions for the case study are as follows:

- **Layer Configuration**—Thick (11-in AC) and thin (4-in AC) sections with material properties (Prony series) at different temperatures
- **Traffic**—3,000 AADTT
- **Growth rate**—1%
- **Loading**—Standard class 9 truck at the maximum loading limits (i.e., 12 kips for steering axle and 34 kips each for two tandem axles)
- **Platoon size**—3
- **Truck speed**—70 mph (maximum speed limit at interstates)
- **Truck spacing**—250 ft (non-platooning) and 60 and 18 ft (platoons). Equivalent to a rest period of 2.5, 0.57, and 0.18 seconds (time headway) in the experimental data.
- **Wander**—Lane width is 12 ft and general truck width is 8 ft. Therefore, trucks can wander 2 ft on either side from the center of the lane. In general, human traffic follows a normal distribution with the center as the mean, with 10 in as standard deviation. However, platoons can be uniformly distributed into sublanes of 2-in width. Three sublanes apart from each other can be used to maximize the potential of lane position optimization (Figure 19) (Okte & Al-Qadi, 2022). The number of platoons distributed at each sublane is equal except for channelized traffic. For example, if the traffic is 300 platoons, then there are 100 platoons per sublane.

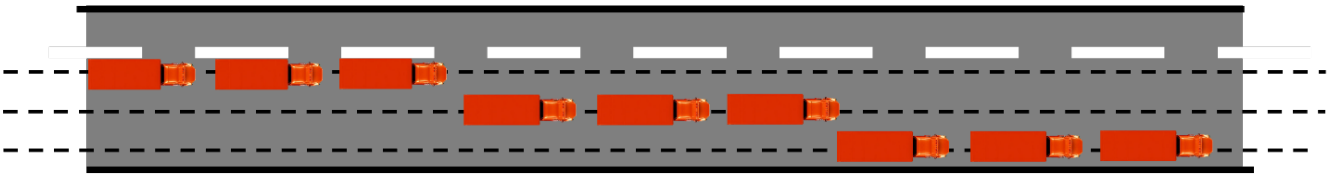

Figure 19. Illustration. Sublanes for reducing pavement damage.

RESULTS

Pavement distresses such as rutting, fatigue, and international roughness index (IRI) progression were calculated by following the methodology. The results can be categorized into two main parts: the effect of penetration level and rest period.

Effect of Platoon Penetration Level

Penetration level (PL) is the percentage of trucks under a platooning scheme. If PL is zero, then the traffic is purely human-driven vehicles, while 100% PL represents completely distributed autonomous vehicles. Channelized traffic represents the condition of fully autonomous traffic but travelling only on a single sublane ([−1,1]). Distresses were the highest for channelized traffic, followed by human traffic, 25%, 50%, 75%, and fully autonomous traffic (Figure 20). Note that Figure 20 represents a platooning scenario where the influence of truck spacing is neglected on the permanent deformation. As the penetration level increases, load application becomes distributed (on sublanes), resulting in lower distresses. Similar trends were observed in the study conducted by Okte and Al-Qadi (2022).

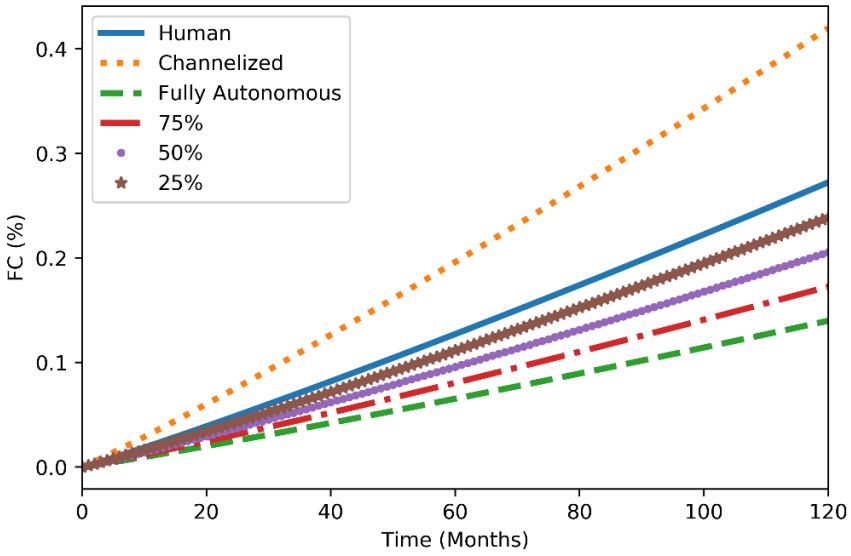

A. Fatigue cracking

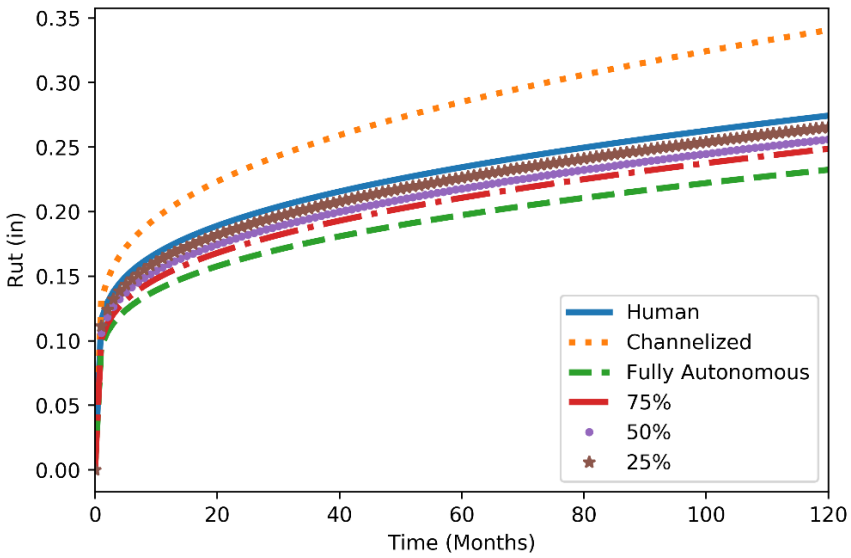

B. Rutting

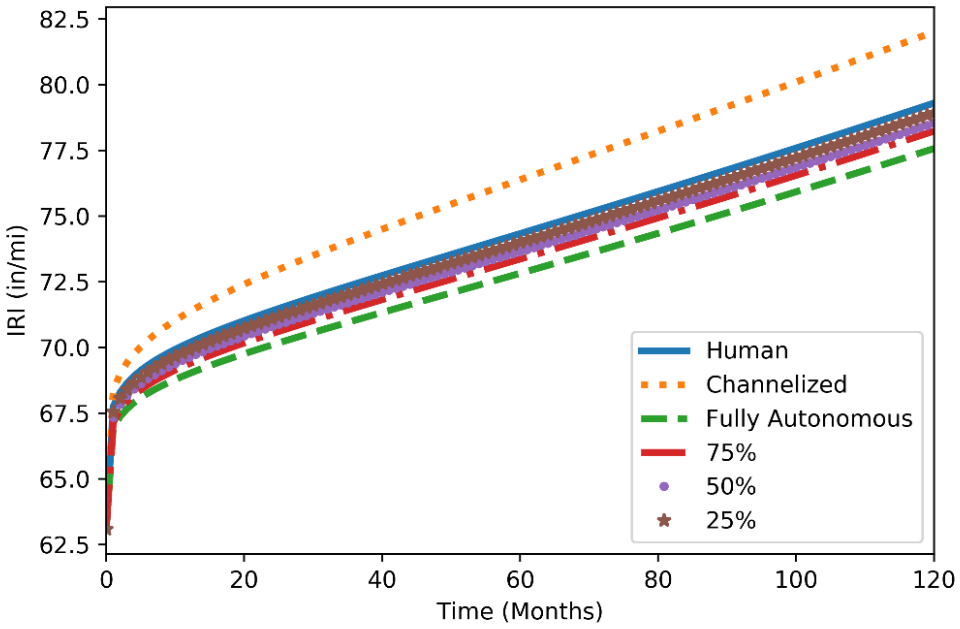

C. IRI

Figure 20. Plots. Distresses at different penetration levels at a rest period of 2.5 seconds.

Effect of Rest Period

As the experimental data were used to incorporate the effect of rest period, rutting of the AC layer is expected to decrease with reduced truck spacing. Theoretically, fatigue cracking increases with reduced spacing. However, based on FE analysis, the tensile strain recovers fully after 0.1 seconds of load application (Al-Qadi et al., 2021). The impact of rest period on fatigue was insignificant when truck spacing is more than 10 ft. The effect of rest period on AC rutting, total rutting, and IRI is presented in Figure 21. Distresses are higher for the 2.5-second rest period, while the difference between 0.18-second and 0.57-second rest periods is insignificant. This observation can be attributed to the experimental results presented earlier (Figure 17). Permanent deformation for the 0.57-second and 0.18-second rest periods were closer and significantly lower compared to deformation at 2.5 seconds. The results of the experimental data were reflected in the distress calculation.

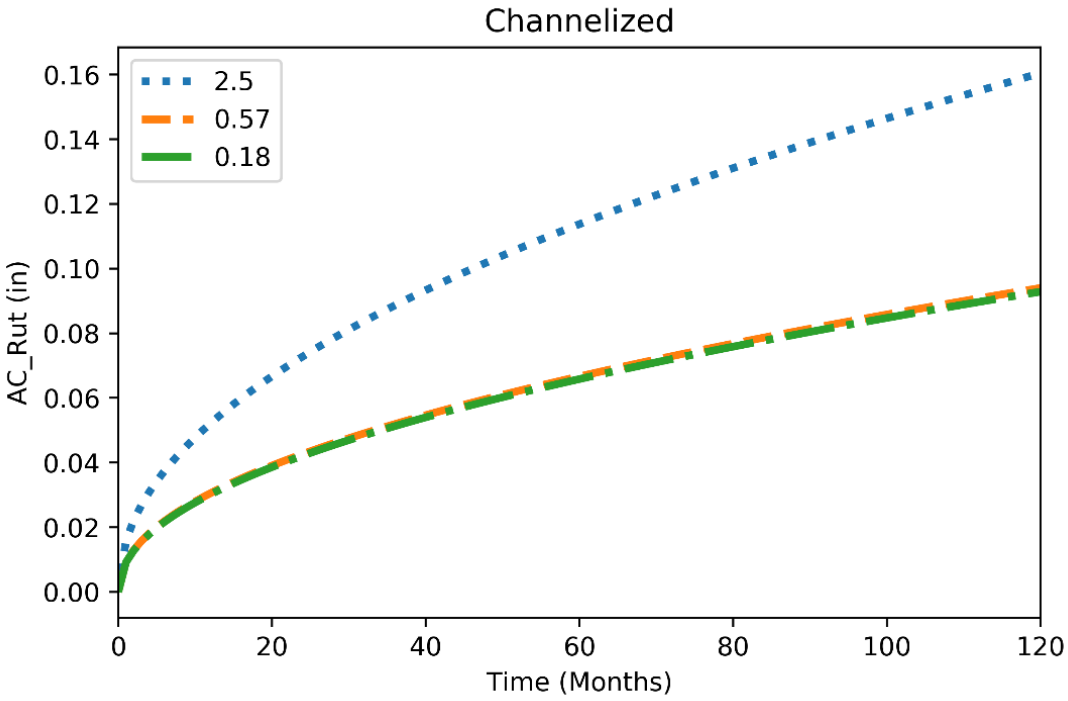

A. AC rutting

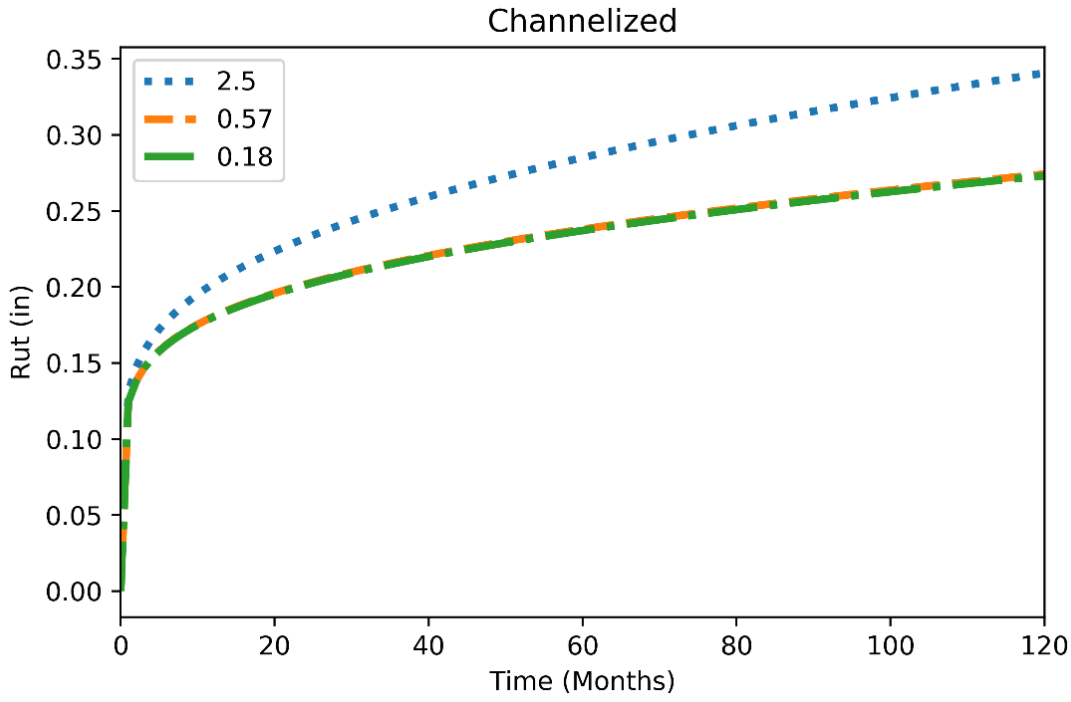

B. Total rutting

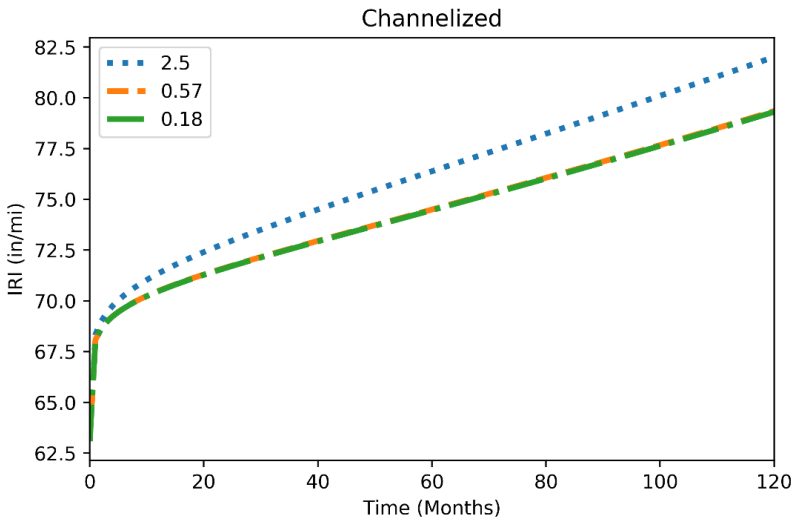

C. IRI

Figure 21. Plots. Effect of rest period for channelized traffic.

Combined Effect

The effect of rest period and penetration level on pavement distresses is straightforward. However, the influence of penetration level will be significantly affected by rest period. In Figure 20, distresses were only presented for a 2.5-second rest period, which simulates the non-platooning scenario. Alternatively, a 2.5-second rest period implies that the effect of rest period is neglected on pavement distresses. In Figure 22, the IRI of channelized traffic is nearly the same as the purely human-driven scenario in contrast with channelized traffic at the 2.5-second rest period. This is mainly due to the reduced equivalent number of repetitions for rest periods compared to 2.5 seconds (non-platooning scenario).

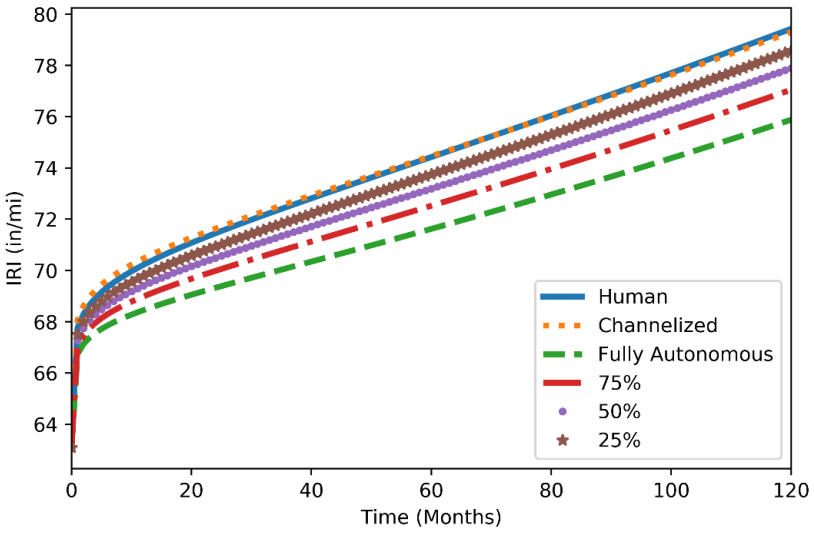

Figure 22. Effect of penetration level at a 0.18-second rest period.

Another important observation is that for the non-platooning scenario, advantages from platooning are not significant after 25% PL. In other words, the gains in the reduction of distress are minimal between fully autonomous traffic and mixed-traffic (25%, 50%, and 75%) conditions. In contrast, for a reduced rest period (0.57 and 0.18 seconds), significant improvements can be observed between fully autonomous and mixed-traffic conditions. At channelized conditions with lower truck spacing, the distresses would be nearly the same or equal to human-driven conditions.

CONCLUSION

Overall, this study highlights and quantifies the importance of truck spacing within a platoon and penetration level in the computation of pavement distresses. Truck platoons are mainly advantageous for the following reasons:

- A reduced rest period plays a significant role in decreasing pavement distresses and enhances the effect of penetration level. Therefore, the previously presented framework can be utilized to compute pavement distresses efficiently.

- In any case, platooning is advantageous even with lower penetration levels. The ideal scenario would be fully autonomous traffic distributed equally on sublanes.

- Though truck spacing of 18 ft resulted in the lowest pavement distresses, the difference in the gains between 60 ft or 18 ft were minimal or insignificant. Hence, 60-ft truck spacing can be considered and would even be preferred over 18 ft because of safety concerns, which are ignored in this study.

CHAPTER 4: SUMMARY AND CONCLUSIONS

The effects of truck platoons on pavement distresses were studied both qualitatively and quantitatively. Rest period is a critical parameter in truck platoon optimization for damage reduction. In a previous study, a reduction in rest period reduced permanent deformation (Ramakrishnan et al., 2021). However, the experiments were limited to conventional triaxial compression and reduced triaxial compression tests. In this study, the experiments were extended to account for representative load pulses of truck platoons to analyze the effect of rest period on permanent deformation. In the experiments, rest period was considered a variable to the stress path. Wander, rest period (i.e., spacing, speed), and penetration levels are key parameters to quantify the effect of platoons on pavements. A framework was developed to compute pavement distresses as a function of all critical variables of truck platoons.

Major findings and conclusions are as follows:

- Conventional triaxial tests with static confinement resulted in higher permanent deformation for higher rest periods. The results are consistent with observations from the previous study (Alrajhi et al., 2022), where no confinement was applied.

- Reduced triaxial compression was found to be a more critical stress state than conventional triaxial stress (path B). Permanent deformation increased consistently with rest period for all stress paths. This finding highlights the necessity to account for variable stress states because of moving loads and rest periods.

- The framework can be used to obtain pavement distress for any rest period, wander, and penetration level. In accordance with the experiments, pavement distresses were lower for lower rest periods. Truck platoons distributed uniformly on sublanes would result in the lowest damage to pavement, even less than conventional trucking.

- As the difference in distresses between 60 ft or 18 ft were insignificant, 60-ft spacing can be considered to alleviate safety concerns, which are ignored in this study.

It is important to add that the initial static stress states used by each stress path were different. The impact of static stresses applied throughout the experiment was not captured in the test results. The impact of static and dynamic stresses should be recorded separately in future experiments to be able to compare stress paths more accurately. To fully capture stress states induced by moving loads, continuous dynamic pulse configurations applied on the vertical and horizontal directions independently will be required.

REFERENCES

AASHTO T 378-17. (2017). Standard method of test for determining the dynamic modulus and flow number for hot mix asphalt using the asphalt mixture performance tester (AMPT). *American Association of State Highway and Transportation Officials.*

Abu Al-Rub, R. K., Darabi, M. K., Huang, C.-W., Masad, E. A., & Little, D. N. (2012). Comparing finite element and constitutive modelling techniques for predicting rutting of asphalt pavements. *International Journal of Pavement Engineering*, *13*(4), 322–338. https://doi.org/10.1080/10298436.2011.566613

Al-Qadi, I. L., & Yoo, P. J. (2007). Effect of surface tangential contact stresses on flexible pavement response. *Journal of the Association of Asphalt Paving Technologists*, *76*(8), 663–692.

Al-Qadi, I., Okte, E., Ramakrishnan, A., Zhou, Q., & Sayeh, W. (2021). *Truck platooning on flexible pavements in Illinois* (FHWA-ICT-21-010). Illinois Center for Transportation. https://doi.org/10.36501/0197-9191/21-010

Alrajhi, A., Ozer, H., & Al-Qadi, I. L. (2022). Impact of rest period on asphalt concrete permanent deformation. *Construction and Building Materials*, *332*, 127329. https://doi.org/10.1016/j.conbuildmat.2022.127329

Ashtiani, R. S. (2009). *Anisotropic characterization and performance prediction of chemically and hydraulically bounded pavement foundations*. Texas A&M University.

Choi, Y.-T., & Kim, Y. R. (2013). Development of calibration testing protocol for permanent deformation model of asphalt concrete. *Transportation Research Record: Journal of the Transportation Research Board*, *2373*(1), 34–43. https://doi.org/10.3141/2373-04

Daniel, J. S., & Kim, Y. R. (2001). Laboratory evaluation of fatigue damage and healing of asphalt mixtures. *Journal of Materials in Civil Engineering*, *13*(6), 434–440. https://doi.org/10.1061/(ASCE)0899-1561(2001)13:6(434)

Darabi, M. K., Abu Al-Rub, R. K., Masad, E. A., & Little, D. N. (2013). Cyclic hardening-relaxation viscoplasticity model for asphalt concrete materials. *Journal of Engineering Mechanics*, *139*(7), 832–847. https://doi.org/10.1061/(ASCE)EM.1943-7889.0000541

Darabi, M. K., Kola, R., Little, D. N., Rahmani, E., & Garg, N. (2019). Predicting rutting performance of flexible airfield pavements using a coupled viscoelastic-viscoplastic-cap constitutive relationship. *Journal of Engineering Mechanics*, *145*(2), 04018129. https://doi.org/10.1061/(ASCE)EM.1943-7889.0001516

Elseifi, M. A., Al-Qadi, I. L., & Yoo, P. J. (2006). Viscoelastic modeling and field validation of flexible pavements. *Journal of Engineering Mechanics*, *132*(2), 172–178. https://doi.org/10.1061/(ASCE)0733-9399(2006)132:2(172)

Epps, J. A., National Cooperative Highway Research Program, National Research Council (U.S.), American Association of State Highway and Transportation Officials, & United States (Eds.). (2002). *Recommended performance-related specification for hot-mix asphalt construction: Results of the WesTrack Project*. National Academies Press.

Fagnant, D. J., & Kockelman, K. (2015). Preparing a nation for autonomous vehicles: Opportunities, barriers and policy recommendations. *Transportation Research Part A: Policy and Practice*, *77*, 167–181. https://doi.org/10.1016/j.tra.2015.04.003

Gibson, N., Schwartz, C., Schapery, R., & Witczak, M. (2003). Viscoelastic, viscoplastic, and damage modeling of asphalt concrete in unconfined compression. *Transportation Research Record*, *1860*(1), 3–15. https://doi.org/10.3141/1860-01

Gungor, O. E., & Al-Qadi, I. L. (2020). All for one: Centralized optimization of truck platoons to improve roadway infrastructure sustainability. *Transportation Research Part C: Emerging Technologies*, *114*, 84–98. https://doi.org/10.1016/j.trc.2020.02.002

Gungor, O. E., & Al-Qadi, I. L. (2022). Wander 2D: A flexible pavement design framework for autonomous and connected trucks. *International Journal of Pavement Engineering*, *23*(1), 121–136. https://doi.org/10.1080/10298436.2020.1735636

Hernandez, J. A., Gamez, A., & Al-Qadi, I. L. (2016). Effect of wide-base tires on nationwide flexible pavement systems: Numerical modeling. *Transportation Research Record: Journal of the Transportation Research Board*, *2590*(1), 104–112. https://doi.org/10.3141/2590-12

Holtz, R. D., Kovacs, W. D., & Sheahan, T. C. (1981). *An introduction to geotechnical engineering* (Vol. 733). Prentice-Hall Englewood Cliffs.

Kim, B., & Roque, R. (2006). Evaluation of healing property of asphalt mixtures. *Transportation Research Record: Journal of the Transportation Research Board*, *1970*(1), 84–91. https://doi.org/10.1177/0361198106197000108

Kim, D., & Kim, Y. R. (2017). Development of stress sweep rutting (SSR) test for permanent deformation characterization of asphalt mixture. *Construction and Building Materials*, *154*, 373–383. https://doi.org/10.1016/j.conbuildmat.2017.07.172

Kim, I. T., & Tutumluer, E. (2005). Unbound aggregate rutting models for stress rotations and effects of moving wheel loads. *Transportation Research Record: Journal of the Transportation Research Board*, *1913*(1), 41–49. https://doi.org/10.1177/0361198105191300105

Kim, Y.-R., Little, D. N., & Lytton, R. L. (2001). Evaluation of microdamage, healing, and heat dissipation of asphalt mixtures, using a dynamic mechanical analyzer. *Transportation Research Record: Journal of the Transportation Research Board*, *1767*(1), 60–66. https://doi.org/10.3141/1767-08

Lambe, T. W., & Whitman, R. V. (1991). *Soil mechanics* (Vol. 10). John Wiley & Sons.

Liang, K.-Y., Martensson, J., & Johansson, K. H. (2016). Heavy-duty vehicle platoon formation for fuel efficiency. *IEEE Transactions on Intelligent Transportation Systems*, *17*(4), 1051–1061. https://doi.org/10.1109/TITS.2015.2492243

Meyers, M. A., & Chawla, K. K. (2008). *Mechanical behavior of materials*. Cambridge university press.

Motevalizadeh, S. M., Ayar, P., Motevalizadeh, S. H., Yeganeh, S., Ameri, M., & bemana, K. (2018). Investigating the impact of different loading patterns on the permanent deformation behaviour in hot mix asphalt. *Construction and Building Materials*, *167*, 707–715.

https://doi.org/10.1016/j.conbuildmat.2018.02.049

Noorvand, H., Karnati, G., & Underwood, B. S. (2017). Autonomous vehicles: Assessment of the implications of truck positioning on flexible pavement performance and design. *Transportation Research Record: Journal of the Transportation Research Board*, *2640*(1), 21–28. https://doi.org/10.3141/2640-03

Okte, E., & Al-Qadi, I. L. (2022). Impact of autonomous and human-driven trucks on flexible pavement design. *Transportation Research Record: Journal of the Transportation Research Board*, 036119812210770. https://doi.org/10.1177/03611981221077083

Praticò, F. G., Casciano, A., & Tramontana, D. (2011). Pavement life-cycle cost and asphalt binder quality: Theoretical and experimental investigation. *Journal of Construction Engineering and Management*, *137*(2), 99–107. https://doi.org/10.1061/(ASCE)CO.1943-7862.0000264

Rahmani, E., Darabi, M. K., Abu Al-Rub, R. K., Kassem, E., Masad, E. A., & Little, D. N. (2013). Effect of confinement pressure on the nonlinear-viscoelastic response of asphalt concrete at high temperatures. *Construction and Building Materials*, *47*, 779–788. https://doi.org/10.1016/j.conbuildmat.2013.05.090

Ramakrishnan, A., Alrajhi, A., Okte, E., Ozer, H., & Al-Qadi, I. (2021). *Truck-platooning impacts on flexible pavements: Experimental and mechanistic approaches* (Report No. ICT-21-038). Illinois Center for Transportation. https://doi.org/10.36501/0197-9191/21-038

Shakiba, M., Gamez, A., Al-Qadi, I. L., & Little, D. N. (2017). Introducing realistic tire–pavement contact stresses into pavement analysis using nonlinear damage approach (PANDA). *International Journal of Pavement Engineering*, *18*(11), 1027–1038. https://doi.org/10.1080/10298436.2016.1141412

Subramanian, V., Guddati, M. N., & Richard Kim, Y. (2013). A viscoplastic model for rate-dependent hardening for asphalt concrete in compression. *Mechanics of Materials*, *59*, 142–159. https://doi.org/10.1016/j.mechmat.2012.10.003

Underwood, B. S., & Zeiada, W. A. (2014). Characterization of microdamage healing in asphalt concrete with a smeared continuum damage approach. *Transportation Research Record: Journal of the Transportation Research Board*, *2447*(1), 126–135. https://doi.org/10.3141/2447-14

Uzan, J. (2003). Characterization of asphalt concrete materials for permanent deformation. *International Journal of Pavement Engineering*, *4*(2), 77–86. https://doi.org/10.1080/10298430310001593272

Witczak, M. W. (2007). Specification criteria for simple performance tests for rutting (Vol. 580). Transportation Research Board.

Witczak, M., & El-Basyouny, M. (2004). Appendix GG-1: Calibration of Permanent Deformation Models for Flexible Pavements. *Guide for Mechanistic–Empirical Design of New and Rehabilitated Pavement Structures*.

Witczak, M. W., Kaloush, K., Pellinen, T., El-Basyouny, M., & Quintus, H. V. (2002). *NCHRP Report—465, Simple Performance Test for Superpave Mix Design*. National Cooperative Highway Research Program, Transportation Research Board.

Yoo, P. J., & Al-Qadi, I. L. (2007). Effect of transient dynamic loading on flexible pavements. *Transportation Research Record: Journal of the Transportation Research Board*, *1990*(1), 129–140. https://doi.org/10.3141/1990-15

Yoo, P. J., Al-Qadi, I. L., Elseifi, M. A., & Janajreh, I. (2006). Flexible pavement responses to different loading amplitudes considering layer interface condition and lateral shear forces. *International Journal of Pavement Engineering*, *7*(1), 73–86. https://doi.org/10.1080/10298430500516074

Zhang, J., Cooley, L., & Kandhal, P. S. (2002). Comparison of fundamental and simulative test methods for evaluating permanent deformation of hot-mix asphalt. *Transportation Research Record: Journal of the Transportation Research Board*, *1789*(1), 91–100. https://doi.org/10.3141/1789-10

Zhou, F., Scullion, T., & Sun, L. (2004). Verification and modeling of three-stage permanent deformation behavior of asphalt mixes. *Journal of Transportation Engineering*, *130*(4), 486–494. https://doi.org/10.1061/(ASCE)0733-947X(2004)130:4(486)